Gain saturation in a Raman-assisted fiber optical parametric amplifier

Xiaojie Guo,* Xuelei Fu, and Chester Shu

Department of Electronic Engineering and Center for Advanced Research in Photonics, The Chinese University of Hong Kong, Shatin, N.T., Hong Kong, China

**Corresponding author: xjguo@ee.cuhk.edu.hk*

Received August 28, 2013; accepted September 13, 2013;
posted September 26, 2013 (Doc. ID 196503); published October 25, 2013

We investigate the gain saturation characteristics in a backward-pumped Raman-assisted fiber optical parametric amplifier (FOPA). It is experimentally observed that the onset of saturation occurs at a higher input power as compared to the case of a conventional FOPA with the same unsaturated gain. The output power under strong saturation is also enhanced. Simulations are performed on the power profile of the parametric pump to explain the distinct saturation behaviors. The monotonic increase of the parametric pump power in the Raman-assisted FOPA results in highly efficient power transfer to the signal while it suppresses the signal conversion to high-order idlers in the saturation regime. © 2013 Optical Society of America

OCIS codes: (060.0060) Fiber optics and optical communications; (060.2320) Fiber optics amplifiers and oscillators; (060.4370) Nonlinear optics, fibers.

http://dx.doi.org/10.1364/OL.38.004405

Fiber optical parametric amplifiers (FOPAs) have attracted much attention because they can provide broadband gain and wavelength conversion over any spectral region when a suitable pump and fiber are available [1]. A major challenge in designing such FOPAs is that the choice of the parametric pump wavelength is limited by the gain bandwidth of erbium-doped fiber amplifiers (EDFAs), which are typically used to amplify the parametric pump to the order of 1 W for a reasonable gain. To overcome this obstacle in designing conventional FOPAs, Raman-assisted FOPAs have been proposed to offer a broad gain bandwidth over 40 THz provided by the Raman pump [2]. With a Raman laser, parametric amplification and wavelength conversion windows have been extended to the S band [3]. In addition, there have been many efforts to achieve gain enhancement up to 27 dB, tailor the gain profile, and optimize the noise figure close to 3 dB [4–7]. Unfortunately, the previous studies focused mostly on the unsaturated (linear gain) but not the saturation regime of Raman-assisted FOPAs.

Gain saturation is an important property of optical amplifiers, especially for FOPAs, which rely on the ultrafast Kerr nonlinearity in fibers. The quasi-instantaneous saturated gain may result in signal distortion during amplification [8,9]. Thus, the maximum input signal power should be carefully controlled within the unsaturated regime. The ultrafast response in gain saturation also makes FOPAs attractive for all-optical signal processing applications, such as phase-preserving amplitude regeneration [10,11]. Gain saturation in conventional FOPAs is attributed to the depletion of pump power [12]. When the input signal power is sufficiently large, the pump power is lessened and the phase mismatch among the interacting fields is changed, resulting in a reduced parametric gain. However, the situation is very different in Raman-assisted FOPAs. A complication arises due to the interplay between the Raman effect and the parametric effect. So far, the characteristics of Raman-assisted FOPAs in the gain saturation regime are largely unexplored.

In this Letter, we investigate the gain-saturation characteristics in a Raman-assisted FOPA. The results are compared to those of a conventional FOPA with an identical unsaturated gain. It is experimentally shown that the signal in the Raman-assisted FOPA starts to saturate at a higher input power. Additionally, a larger output power is obtained in strong saturation. The observations are analyzed by numerically solving the nonlinear Schrödinger equation (NLSE) with the inclusion of the Raman effect. The simulation results reveal that in the gain-saturation regime, the Raman gain compensates the depletion of the parametric pump caused by a strong signal input. The change in the power evolution of the parametric pump thus leads to new and different gain saturation characteristics in Raman-assisted FOPAs.

First, the gain saturation effect in a Raman-assisted FOPA is experimentally observed. Our setup is depicted in Fig. 1. A continuous-wave (CW) tunable laser (TL1) is used as the parametric pump at a wavelength of 1555 nm. The CW pump is phase modulated by a 10 Gb/s $2^7 - 1$ PRBS to suppress stimulated Brillouin scattering in the fiber. The pump is then amplified, followed by a 1-nm OBPF to reduce the amplified spontaneous emission noise generated from the EDFA. Another CW tunable laser (TL2) serves as the signal at a wavelength of 1545.5 nm. The signal power can be adjusted by a VOA in the experiment. The pump and signal are combined by a 75/25 coupler, and their polarization states

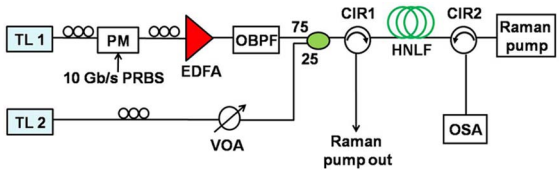

Fig. 1. Experimental setup of the Raman-assisted FOPA. TL, tunable laser; PM, phase modulator; PRBS, pseudorandom binary sequence; EDFA, erbium-doped fiber amplifier; OBPF, optical bandpass filter; CIR, optical circulator; VOA, variable optical attenuator; HNLF, highly nonlinear fiber; OSA, optical spectrum analyzer.

are optimized at the input of the HNLF by two PCs. The HNLF has a length of 1 km, a nonlinear coefficient $\gamma = 11.7\ \mathrm{W^{-1}\,km^{-1}}$, and a Raman gain coefficient $\gamma_R = 3.8\ \mathrm{W^{-1}\,km^{-1}}$. The zero dispersion wavelength (ZDW) is 1549 nm. The dispersion, dispersion slope, and attenuation coefficient at 1550 nm are $0.02\ \mathrm{ps\cdot km^{-1}\,nm^{-1}}$, $0.019\ \mathrm{ps\cdot km^{-1}\,nm^{-2}}$, and $0.79\ \mathrm{dB\,km^{-1}}$, respectively. At the HNLF output, a 1455-nm CW fiber laser acting as the Raman pump is launched into the HNLF in the opposite direction. The Raman gain peak is located at 1554 nm. The amplified signal is extracted from the HNLF through an optical circulator (CIR2) and then analyzed by an OSA.

Figure 2 shows the on–off gain obtained by measuring the output signal powers with the pumps turned on and turned off. The unsaturated on–off gain of the Raman-assisted FOPA is 28 dB with a 21.7 dBm parametric pump and a counterpropagating Raman pump of 30.4 dBm. The parametric pump provides a 3 dB small-signal gain when the Raman pump is turned off. The Raman pump works in the saturation regime and offers an on–off Raman gain of 8.9 dB for the parametric pump. As the input signal power increases, a moderate saturation (2 dB gain drop) is found at an input level of −5 dBm. To draw the comparison with a conventional FOPA, the gain saturation is also studied with a 26.2 dBm parametric pump but without a Raman pump. Both types of FOPAs are set to have the same on–off gain in the linear regime, as shown in Fig. 2. The gain of the conventional FOPA starts to saturate at a lower signal input power. It has a 2 dB gain drop at an input signal power, which is 4 dB lower than that of the Raman-assisted FOPA. In the saturation regime, the on–off gain of the Raman-assisted FOPA is larger than that of the conventional FOPA. An increasing gain difference between the two FOPAs is observed as the input power increases.

The saturation behaviors are also characterized in terms of the relation between the output and the input signal powers. As shown in Fig. 3, under strong saturation, the output signal of the Raman-assisted FOPA reaches a maximum power that is 5 dB higher than that of the conventional FOPA. It is important to mention that the sum of the individual gains of the Raman pump and the parametric pump is lower than the gain obtained in the Raman-assisted FOPA. Hence, the enhancement of the output level under the saturation condition cannot be simply ascribed to direct Raman amplification. It should be noted that the signal wavelength under study is located at the gain peak of the conventional FOPA, which happens to be close to that of the Raman-assisted FOPA at 1546.5 nm. Therefore, the difference of the saturation behaviors between the two FOPAs cannot

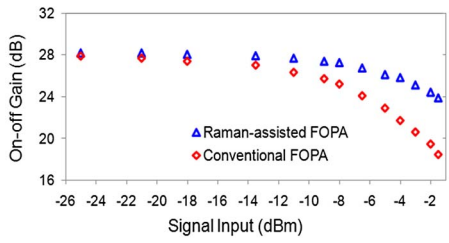

Fig. 2. On–off gain of the Raman-assisted FOPA and the conventional FOPA as a function of the input power.

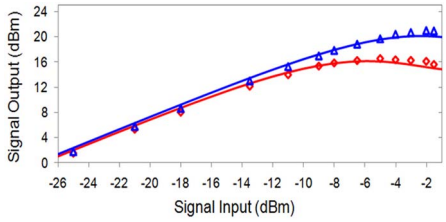

Fig. 3. Output signal power against the input. Blue triangles and red diamonds are experimental data obtained from the Raman-assisted FOPA and the conventional FOPA, respectively. Blue and red solid curves are simulation results.

be explained by the wavelength dependence of gain saturation with respect to the gain peak wavelength as reported in [12].

To understand the physical mechanism behind the gain saturation of the Raman-assisted FOPA, theoretical calculations have been carried out to investigate the interaction among the waves propagating along the HNLF. In the Raman-assisted FOPA, the signal is amplified through both the Raman effect and the parametric effect. At the same time, the parametric pump is also amplified by the Raman pump. The signal is amplified mostly through the parametric process because the nonlinear coefficient γ is about 3 times that of the Raman coefficient γ_R. In the following theoretical model, since the wavelength of the Raman pump is far from the ZDW of the HNLF, we can neglect the parametric processes involving the Raman pump. Thus, the nonlinear interaction among all the waves can be simplified to only two processes: the direct Raman amplification of the Stokes waves (including the parametric pump, signal, and generated idlers), and the parametric interaction among the Stokes waves.

By assuming that the Raman gain is wavelength independent, the power coupling from the counterpropagating Raman pump to the Stokes waves can be described by the following set of equations [13]:

$$\frac{dP_{\mathrm{Stokes}}}{dz} = -\alpha P_{\mathrm{Stokes}} + \gamma_R P_R P_{\mathrm{Stokes}}, \tag{1a}$$

$$\frac{dP_R}{dz} = \alpha_R P_R + (\lambda_{\mathrm{Stokes}}/\lambda_R)\gamma_R P_{\mathrm{Stokes}} P_R, \tag{1b}$$

where P_{Stokes} is the power of the Stokes waves, P_R is the Raman pump power, and α and α_R are the attenuation coefficients of the Stokes and Raman pump waves. The assumption of a flat Raman gain is suitable because the dominant Stokes waves (the pump, signal, and idler) occupy a relatively narrow wavelength range with respect to the Raman gain bandwidth. Under this assumption, a power profile $P_R(z)$ of the Raman pump can be obtained by solving Eqs. (1) with the initial condition that $P_{\mathrm{Stokes}}(0)$ represents the power sum of the signal and the parametric pump power launched into the HNLF.

Next, the parametric process can be simulated by numerically solving the NLSE using the split-step Fourier method [14]. The NLSE has the form

$$\frac{\partial A}{\partial z} - \sum_{n=1}^{4} \frac{i^{n+1}\beta_n}{n!}\frac{\partial^n A}{\partial t^n} + \frac{\alpha}{2}A = i\gamma|A|^2 A + \frac{\gamma_R}{2}P_R A, \qquad (2)$$

where $A(z,t)$ is the sum of the complex envelopes of all waves involved in the parametric process, and β_n is the nth derivative of the propagation constant $\beta(\omega)$ with respect to ω. On the right-hand side of Eq. (2), the first term corresponds to the parametric effect while the second term corresponds to the Raman effect. This approach is appropriate in describing the parametric process, particularly in the saturation regime because all the waves including the created high-order idlers are considered by the NLSE. In the simulation, the power profile $P_R(z)$ obtained from Eq. (1) is substituted into Eq. (2) to calculate the Raman gain. The simulation results in Fig. 3 are in good agreement with the experimental data.

Using the above theoretical model, we analyze the evolution of the parametric pump power as well as the signal gain along the fiber. Figure 4(a) shows the result at an input signal power of −25 dBm located in the unsaturated regime. There is a distinct difference between the two types of FOPAs even though they achieve the same final signal gain. For the conventional FOPA, the gain expressed in dB varies along the HNLF with a constant gain slope resulting from the nearly unchanged pump power. However, in the Raman-assisted FOPA, the parametric pump is amplified by the Raman pump along the HNLF. Accordingly, the signal is amplified with an increasing gain slope.

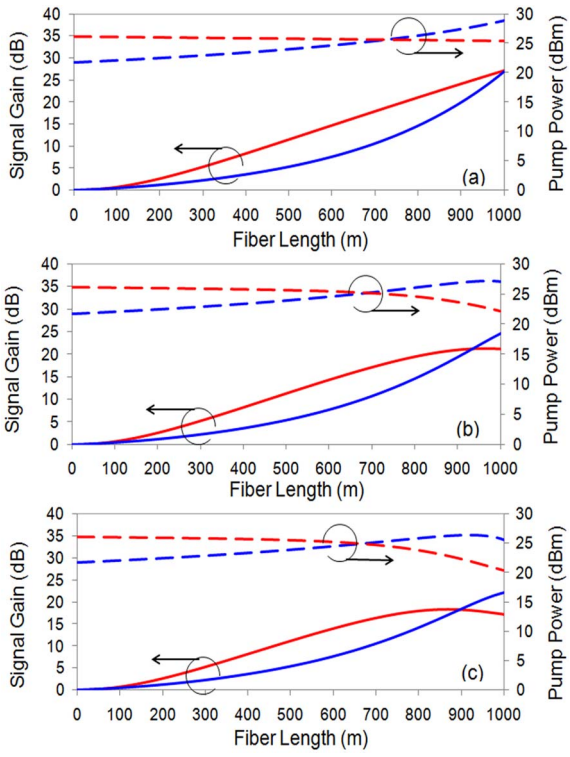

Fig. 4. Profiles of the parametric pump power and the signal gain along the fiber for an input signal power of (a) −25 dBm, (b) −5 dBm, and (c) −2 dBm. Blue and red curves are the results of the Raman-assisted FOPA and the conventional FOPA, respectively.

The interesting properties of gain saturation in the Raman-assisted FOPA can be ascribed to the unique power evolution of the parametric pump. Here, we calculate the parametric power and the signal gain as a function of the distance along the HNLF under the saturation condition. Figure 4(b) shows the results with an input signal power of −5 dBm. The output of the conventional FOPA reaches a peak, while the Raman-assisted FOPA is still in moderate saturation. The parametric pump in the Raman-assisted FOPA is progressively amplified by the Raman pump, although the power-rising slope is smaller than that in the linear-gain regime. This is because the signal takes away more energy from the parametric pump when the input signal level is higher. Nevertheless, the signal gain still rises with an increasing gain slope, similar to the case of unsaturated gain. This behavior is not observed in the conventional FOPA. Without the Raman amplification in the FOPA, the parametric pump power is quickly reduced. Consequently, the signal gain stops ascending near the output port of the HNLF.

As the input signal is further raised to −2 dBm, as shown in Fig. 4(c), the gain of a conventional FOPA begins to drop near the output end. On the contrary, the Raman gain compensates the parametric pump depletion in the Raman-assisted FOPA, and thus the signal gain reaches a higher level under strong saturation. The results clearly indicate that the power transfer to the signal is more efficient in the Raman-assisted FOPA due to a monotonic increase of the parametric pump power.

Apart from pump depletion, the generation of high-order idlers also causes saturation of the output signal in FOPAs [15]. At sufficiently high powers of the signal and primary idler, a new idler will be generated through the parametric process that satisfies $f_s + f_p = f_i + f_{\mathrm{hi}}$, where f_s, f_p, f_i, and f_{hi} are the frequencies of the signal, pump, idler, and high-order idler. Therefore, the high-order idler grows at the expense of the signal power. Figure 5 illustrates the output spectra of the Raman-assisted FOPA and the conventional FOPA at a signal input of −8 dBm. It is noted that the signal gains are reduced by 0.9 and 2.7 dB from the small-signal linear gains for the respective cases of the Raman-assisted FOPA and the conventional FOPA, as can be derived from Fig. 2.

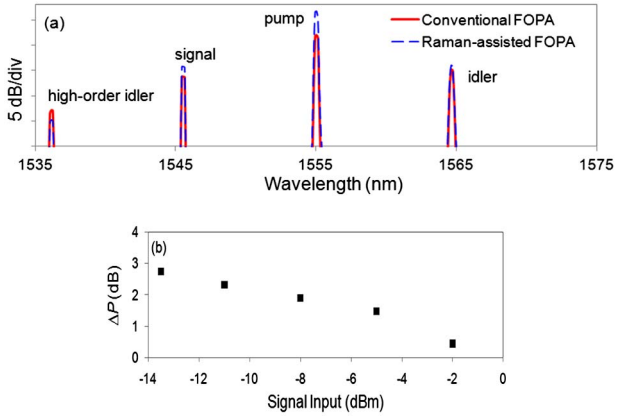

Fig. 5. (a) Output spectra at an input signal power of −8 dBm. (b) Power difference between the high-order idlers obtained from the Raman-assisted FOPA and the conventional FOPA as a function of the input signal power.

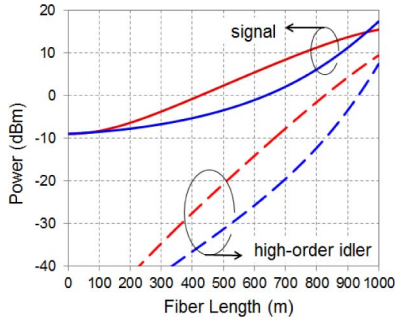

Fig. 6. Power profiles of the signal and the high-order idler along the fiber. The input signal power is −8 dBm. The blue and red curves are the results of the Raman-assisted FOPA and the conventional FOPA, respectively.

A high-order idler appears at 1536 nm for both types of FOPAs. The idler power in the Raman-assisted FOPA is 2 dB lower than that in the conventional FOPA. The measured output power difference of the high-order idler between the two FOPAs ΔP is shown in Fig. 5(b). The values are larger than 0 dB, which implies that the high-order idler consumes less power from the signal in the Raman-assisted FOPA. Thus, the saturation of the output signal is deferred. Since the power of the high-order idler is influenced by that of the signal, the power profiles of the two components are simulated to analyze the phenomenon. The results are shown in Fig. 6. We observe that the signal power is lower than that in the conventional FOPA until the last 50 m of the HLNF. Consequently, the high-order idler of the Raman-assisted FOPA remains at a smaller power along the HLNF. The special power evolution of the signal leads to a lower output power of the high-order idler.

In deeper saturation, new high-order idlers are generated and the power transfer processes become complicated. Nevertheless, the powers of the new high-order idlers are dependent on that of the first high-order idler, f_{hi}. Accordingly, the high-order idlers will be weaker for the Raman-assisted FOPA, resulting in a higher output signal power. With the generation of high-order idlers, the assumption of a uniform Raman gain in the theoretical model will lead to a disagreement between the simulation and the experimental results. To obtain a more accurate simulation, one should use the general NLSE including the delayed nonlinear response [14].

In summary, gain saturation in a backward-pumped Raman-assisted FOPA has been investigated by drawing the comparison with a conventional FOPA of the same linear gain. Different saturation characteristics have been experimentally observed and analyzed. The Raman-assisted FOPA saturated at a higher input power and produced a larger output under strong saturation compared to the conventional FOPA. A theoretical model based on the NLSE has been used to simulate the interplay of the Raman effect and parametric effect in analyzing the saturation behaviors. The unusual saturation in the Raman-assisted FOPA is attributed to a monotonic increase of the parametric pump power along the HNLF due to the Raman amplification. Such a power evolution changes the efficiencies of the power transfer to the signal and to the high-order idler. The higher transfer efficiency from pump to signal, together with the lower efficiency from signal to high-order idler lead to slower gain saturation and higher signal output in the Raman-assisted FOPA. Such saturation behaviors in the Raman-assisted FOPA offer potential advantages over the conventional FOPA. For instance, in optical amplification, the slow gain saturation allows an increase in the maximum input signal power without causing distortion. Additionally, in optical regeneration utilizing the strong saturation, the higher output signal level can reduce the penalty caused by a finite signal extinction ratio.

This work was supported by a GRF grant (CUHK 416509) and a CUHK direct grant.

References

1. T. Torounidis and P. Andrekson, IEEE Photon. Technol. Lett. **19**, 650 (2007).
2. M. N. Islam, IEEE J. Sel. Top. Quantum Electron. **8**, 548 (2002).
3. J. F. L. Freitas, M. B. Costa e Silva, S. R. Lüthi, and A. S. L. Gomes, Opt. Commun. **255**, 314 (2005).
4. S. Peiris, N. Madamopoulos, N. Antoniades, M. Ummy, M. Ali, and R. Dorsinville, Appl. Opt. **51**, 7834 (2012).
5. H. K. Y. Cheung, K. K. Y. Wong, N. Wong, and M. E. Marhic, Proc. SPIE **6103**, 61030S1 (2006).
6. S. H. Wang, L. Xu, and P. K. A. Wai, in *Proceedings of the IEEE Conference on Opto-Electronics and Communications* (IEEE, 2009).
7. S. H. Wang, L. Xu, P. K. A. Wai, and H. Y. Tam, J. Lightwave Technol. **29**, 1172 (2011).
8. F. Da Ros, R. Borkowski, D. Zibar, and C. Peucheret, in *European Conference and Exhibition on Optical Communication*, OSA Technical Digest Series (Optical Society of America, 2012), paper We.2.A.3.
9. Z. Lali-Dastjerdi, F. Da Ros, K. Rottwitt, M. Galili, and C. Peucheret, in *Proceedings of IEEE Conference on Lasers and Electro-Optics* (IEEE, 2012).
10. M. Matsumoto and T. Kamio, IEEE J. Sel. Top. Quantum Electron. **14**, 610 (2008).
11. M. Gao, J. Kurumida, and S. Namiki, Opt. Lett. **35**, 3468 (2010).
12. K. Inoue and T. Mukai, Opt. Lett. **26**, 10 (2001).
13. J. Bromage, J. Lightwave Technol. **22**, 79 (2004).
14. G. P. Agrawal, *Nonlinear Fiber Optics*, 4th ed. (Academic, 2006).
15. K. Inoue, IEEE Photon. Technol. Lett. **13**, 338 (2001).